Regular Article

The behaviour of vascular smooth muscle cells and platelets onto epigallocatechin gallate-releasing poly(L-lactide-*co*-ε-caprolactone) as stent-coating materials

Han Hee Cho, Dong-Wook Han, Kazuaki Matsumura, Sadami Tsutsumi, Suong-Hyu Hyon*

Department of Medical Simulation Engineering, Research Center for Nano Medical Engineering, Institute for Frontier Medical Sciences, Kyoto University, Kyoto 606-8507, Japan

*Corresponding author. Department of Medical Simulation Engineering, Research Center for Nano Medical Engineering, Institute for Frontier Medical Sciences, Kyoto University, 53 Kawahara-cho, Shogoin, Sakyo-ku, Kyoto 606-8507, Japan. Tel.: +81 75 751 4125 (direct); fax: +81 75 751 4141. *E-mail address:* biogen@frontier.kyoto-u.ac.jp (S.-H. Hyon).

1. Introduction

Neointimal hyperplasia is principally responsible for in-stent restenosis and remains an important clinical problem in the treatment of vascular occlusions. Stent material and surface properties are key determinants in the formation of acute thrombus and in-stent restenosis [1]. Commonly used bare metal stents offer excellent mechanical stability, but often increase the incidence of inflammation, thrombosis, fibromuscular proliferation and formation of restenosis [1,2]. Recently, drug-eluting stents (DES), which have synthetic polymer coatings that act as drug reservoirs and elute drugs over a period of several weeks or months, have emerged [3–6]. These DES can provide luminal scaffolding that virtually eliminates recoil and remodeling of the treated vessel. Additionally, the polymer coatings contain drugs that inhibit thrombus formation, inflammation or vascular smooth muscle cell (VSMC) proliferation [5]. After the drug elutes from the polymer coatings, the residual synthetic polymer coatings remain in place. Eventually, the permanent presence of the nonresorbable polymer may lead to complications, such as an exaggerated inflammatory response and neointima formation, at the implant site [7,8]. It is, therefore, desirable to develop DES not only with a biocompatible and biodegradable coating to prevent these unfavorable effects, but also loaded with effective drugs that either promote re-endothelization or suppress inflammation and VSMC proliferation [9,10].

Our attention has been paid to (–)-epigallocatechin-3-*O*-gallate (EGCG), a main polyphenolic component of green tea, since it has a wide range of pharmacological activities, including antioxidant, anti-proliferative, anti-inflammatory, anti-atherogenic and anti-thrombotic effects [11–14]. Biodegradable copolymers, such as poly(lactide-*co*-ε-caprolactone, PLCL) and poly(glycolide-*co*-ε-caprolactone), have been shown to possess vascular tissue compatibility, flexible and rubber-like elasticity and proper degradability

[15,16]. Our earlier study has already shown that EGCG inhibits the proliferation and migration of serum-stimulated VSMCs *in vitro* and induces cell cycle arrest via nuclear factor-κB down-modulation [17]. In this study, we hypothesized that loading EGCG in coating of DES can make the in-stent restenosis, thrombosis and inflammation decrease significantly by inhibiting the migration and invasion of VSMCs as well as the adhesion and activation of platelets. EGCG releasing PLCL films were prepared and their various in vitro physicochemical characteristics, drug release profiles and in vitro blood compatibility are investigated.

2. Materials and methods

2.1. Preparation of EGCG-releasing PLCL

PLCL [75:25 (mol/mol), molecular weight (MW) 130 ~ 150 kDa] resin used in this study was kindly provided by BMG Inc. (Kyoto, Japan). EGCG-releasing PLCL (E-PLCL) was prepared by solvent casting. PLCL resins were dissolved in acetone at 60°C and blended with 5 wt% EGCG (MW 458.4, Teavigo™, DSM Nutritional Products Ltd., Basel, Switzerland). The mixtures were cast on glass Petri dishes and allowed to dry solvent slowly at room temperature overnight. Next the cast films were put under a vacuum to evaporate residual solvent for 2 days, resulting in smooth and non-porous films. PLCL and E-PLCL films were cut into a disc of 10 mm in diameter and 100 μm in thickness. These discs weighed about 10 mg, unless otherwise specified. Thus, approximately 500 μg (≈ 1.1 mmol) EGCG was loaded in one E-PLCL disc. In order to examine VSMC behaviors onto E-PLCL films and their anti-thrombotic activity, the films were sterilized with ethylene oxide gas and adhered onto the bottom of well plates by using sterile vacuum grease.

2.2. Physicochemical characterization

2.2.1. Scanning electron microscopy (SEM)

The surface morphologies of PLCL and E-PLCL films were examined under a field emission scanning microscope (Hitachi S–800, Tokyo, Japan). The films were mounted and sputter-coated with gold using an ion coater and then observed at an accelerating voltage of 20 kV.

2.2.2. Differential scanning calorimetry (DSC)

The endothermic scans of PLCL and E-PLCL films were obtained by DSC, using a scanning rate of 10°C/min from 25 to 300°C. A DSC–3100SA (MAC Science Co., Ltd., Yokohama, Japan) system connected to a low-temperature refrigerator system (Intracooler II) was used. Liquid nitrogen was used to purge the film head and glove box. The instrument was calibrated using aluminum at the same scanning rate as the films (≈ 2 mg). All DSC runs were repeated in triplicate. For comparison, the endothermic profile of free EGCG was also scanned.

2.2.3. Attenuated total reflectance/Fourier transformed-infrared (ATR/FT-IR) spectroscopy

The infrared spectra of PLCL and E-PLCL films were obtained between 4,150 and 650 cm^{-1} using an ATR/FT-IR spectrophotometer (Spectrum one FT-IR Spectrometer, Perkin–Elmer, Boston, MA).

2.2.4. Water contact angle

To compare the hydrophilicity of E-PLCL with that of PLCL, water contact angles were examined by the sessile droplet method. The contact angles of water onto PLCL and E-PLCL films were measured at room temperature using a contact angle meter (Model CA–X, Kyowa Interface Science Co., Ltd., Saitama, Japan) equipped with a special optical system and a charge-coupled device camera.

2.3. In vitro release profile of EGCG from E-PLCL

E-PLCL films were adhered to the bottom of a glass vial by using sterile vacuum grease and then incubated in phosphate-buffered saline (PBS, pH 7.4) at 37°C for up to 34 days. At the end of each predetermined incubation period, the absorbance at 275 nm was quantified using a UV spectrophotometer (U–2800A, Hitachi, Tokyo, Japan). The concentration (μM) of EGCG released from E-PLCL was calculated from the standard calibration curve of EGCG solution.

2.4. In vitro degradation

MW change (%) and cumulative weight loss (%) were used as indices of PLCL degradation. PLCL and E-PLCL films were cut into 15 mm × 5 mm (100 μm in thickness) and weighed respectively using an analytical balance. Weighed films were immersed in 3 ml of PBS and incubated in a bioshaker (BR–4OLF, Taitec, Saitama, Japan) at 37°C with shaking at 60 rpm for up to 8 weeks. The PBS was refreshed every week. At determined time intervals, films were retrieved, washed with distilled water and dried in a vacuum desiccator for 24 h at room temperature. Immediately after vacuum-drying, the MW of PLCL was measured by gel permeation chromatograph system (GPC, HLC–8020, Toyo soda, Tokyo,

Japan) with a refractive detector and TSK gel G5000HXL and G3000HXL columns. Polystyrene standards were used for calibrating MW. The mass loss of PLCL and E-PLCL films was determined as percentage (%) of the dry weight of each film at each time divided by its initial dry weight.

2.5. VSMC culture

VSMCs were isolated by limited enzymatic digestion from the tunica media of thoracic aorta of male adult (10 week old) Sprague Dawley rats (280 ~ 300 g in weight, Shimizu Laboratory Supplies, Kyoto, Japan) as previously reported [18]. The primarily cultured VSMCs were cultured in a complete Dulbecco's modified Eagle's medium (DMEM, Sigma–Aldrich Co., St. Louis, MO), supplemented with 10% fetal bovine serum (FBS, Sigma–Aldrich) and 1% antibiotic antimycotic solution (including 10,000 units penicillin, 10 mg streptomycin and 25 μg amphotericin B per ml, Sigma–Aldrich) at 37°C and 5% CO_2 in a humid environment. Studies were performed with the cells between the third to seventh passage.

2.6. VSMC migration and invasion assays

Using a method similar to that previously described [19], *in vitro* migration assay was performed. Briefly, VSMCs (2×10^4 cells/ml) were seeded into 48-well plates, where PLCL films had been placed on the bottom of wells, and then grown to confluence. Monolayers were scraped (denuded) using a 1 ml plastic micropipette tip and replaced with conditioned media obtained by incubating either PLCL or E-PLCL in complete DMEM for 72 h, followed by incubation in a CO_2 incubator. The cells, that migrated toward denuded space for 72 h,

were visualized by immuno-cytochemical analysis using mouse monoclonal anti-α-smooth muscle actin (SMA) antibody (Clone 1A4, Sigma–Aldrich) conjugated with FITC isomer I and propidium iodide (5 μM, Sigma–Aldrich), counterstaining agent for cell nuclei. These cultures were then examined under a fluorescence microscope (Biozero–8000, Keyence, Osaka, Japan) using a modified method as previously described [20]. The average area covered by migrated cells was calculated by using an image processing software (BZ analyzer Ver. 2.5, Keyence).

An invasion assay was performed *in vitro* using a modified Boyden chamber assay [21]. Briefly, the membrane (8.0 μm pore size) of transwell inserts (Nunc, Rochester, NY) was coated with 20 μl of matrigel solution (1 mg/ml) in DMEM for 12 h at 4°C and then rinsed twice with PBS. VSMCs were seeded in the inner chamber of transwell at 5×10^4 cells/well and given 300 μl of conditioned media obtained by incubating either PLCL or E-PLCL for 72 h in a serum-free DMEM. The lower chamber was filled with 500 μl of a complete DMEM and incubated for 72 h at 37°C in a CO_2 incubator. After incubation, all the non-migrant cells were removed from the upper face of the transwell membrane with a cotton swab and migrant cells were stained with 0.5% toluidene blue solution. The number of cells that had invaded through the membrane was counted in six randomly chosen fields of each transwell by using an inverted microscope (IX70, Olympus Optical Co., Osaka, Japan).

2.7. Platelet adhesion and activation assays

Platelet adhesion and activation were employed as indices of the anti-thrombotic effects of E-PLCL. Human whole blood was collected into a polypropylene syringe containing acid citrate dextrose A (an anticoagulant solution, 1/6 volume of blood). The upper platelet-rich

plasma (PRP) layer was obtained by centrifuging whole blood at 1000 rpm for 10 min. Both films were immersed in PBS for 30 min to equilibrate the surface and then incubated with PRP for 2 h at 37°C. The films were washed with PBS three times to remove non-adherent platelets and soaked in 2.5% glutaraldehyde (Sigma–Aldrich) for 2 h to fix adhered platelets. After washing with PBS, the films were dehydrated in a graduated ethanol solution for 5 min each (50 ~ 100%) and dried in a desiccator at room temperature. The platelet-adhered surfaces were sputter-coated with gold using an ion coater and then examined by SEM (Hitachi S–800) at an accelerating voltage of 10 kV. The number of adhered platelets was counted from SEM micrographs with higher magnification (×1000).

Platelet activation was investigated by determining soluble P-selectin (CD62) with an enzyme immunoassay kit (Takara Bio Inc., Tokyo, Japan). According to the manufacturer's instructions, PRP, following incubation with either PLCL or E-PLCL film, was added to a 96-well plate coated with mouse monoclonal anti-CD62 antibody and then incubated for 2 h at room temperature. Standard P-selectin (0, 10, 20, 40, 80, 160 and 320 ng/ml) was also reacted. To block nonspecific antibody binding, the wells were blocked with 1% bovine serum albumin (Sigma–Aldrich) in PBS for 30 min at room temperature. After rinsed three times with PBS, the wells were incubated with peroxidase-conjugated anti-mouse secondary antibody for 1 h at room temperature. Hydrogen peroxide/tetramethylbenzidine substrate agent was added to the wells for color development and further incubated for 15 min. Afterwards, the enzyme reaction was stopped by the addition of 1N H_2SO_4, and absorbance was determined at 450 nm with a microplate reader (VersaMax™, Molecular Devices Co., Sunnyvale, CA).

2.8. Preparation of EGCG-eluting stents and balloon-expansion test

Stents (17 mm in length, 1.6 mm in diameter) consisting of Co-Cr alloy were kindly donated by Japan Stent Technology Co. Ltd. (Okayama, Japan). PLCL and EGCG were dissolved in acetone to yield a solution of 0.5 wt% (0.475% and 0.025%, respectively). The PLCL solution containing EGCG was sprayed onto the surface of stents using an ultrasonic spray-coating method with stent coating system (MediCoat™ DES 1000, Sono–Tek Co. Ltd., Milton, NY). The mass of the coating sprayed onto the stent surface was obtained by weighing the stent before and after spraying. The coating weight for a stent was approximately 620 μg, and the resulting drug content was about 30 μg. The surface morphology of EGCG-eluting stents before and after balloon-expansion was examined with digital microscope (VHX–100, Keyence). The layer quality and structural integrity of E-PLCL coating after balloon-expansion were examined by SEM (Shimazu SS–550). The stent was mounted onto an angioplasty balloon and the balloon was dilated to 3.0 mm at a pressure of 20 atm.

2.9. Statistical analysis

All variables were tested in three independent cultures for each experiment, and each experiment was repeated twice (n = 6). Quantitative data is expressed as mean ± standard deviation (SD). Statistical comparisons were carried out with a one-way analysis of variance (ANOVA, SAS Institute Inc., Cary, NC, USA), which was followed by the Bonferroni test for the multiple comparisons. A value of $p < 0.05$ was considered statistically significant.

3. Results

3.1. Physicochemical characteristics of E-PLCL

E-PLCL was prepared by blending PLCL with 5 wt% EGCG which induced a red-color because of EGCG addition. The physicochemical properties of PLCL and E-PLCL films were examined by SEM, DSC, FT-IR spectroscopy and water contact angle. SEM demonstrated that the surface morphology and roughness of E-PLCL (Fig. 1A) was almost similar to those of PLCL. The DSC profiles showed that the melting temperature (Tm) of PLCL was slightly lowered to 153.5°C from 154.2°C by EGCG impregnation (Fig. 1B). The conversion T of EGCG into GCG, its epimer, was near 97°C (a, the insert of Fig. 1B). The Tm of GCG was at 223°C (b), the crystallization T of EGCG was at 235°C (c) and the Tm of EGCG was at 246°C (d). This result suggests that EGCG addition might not affect the crystallinity of PLCL.

FT-IR spectrum of E-PLCL was dominated by a broad noticeable band at 3,600 ~ 3,150 cm^{-1}, which is the characteristic peak of phenyl – OH groups abundant in EGCG (Fig. 2A, top). Additionally, the characteristic bands of EGCG were found at 1610 cm^{-1} for C = C alkenes and at 823 cm^{-1} for C – H alkenes (Fig. 1C, bottom). Strong peaks of PLCL and E-PLCL near 1750 cm^{-1} were derived from the carbonyl stretching (C = O) of the PLA and PCL block. Furthermore, the characteristic peaks of EGCG were not shifted in E-PLCL. Therefore, it seemed that EGCG might be well dispersed in E-PLCL film. To compare the hydrophilicity of PLCL with that of E-PLCL, the water contact angles were measured using the sessile droplet method. The water contact angle of PLCL was 83.8±1.8° and that of E-PLCL was 78.2±1.6°. These results showed that the hydrophilicity of PLCL was significantly ($p < 0.05$) increased, which was attributed to the presence of hydrophilic groups in EGCG.

3.2. EGCG release from E-PLCL and effects of EGCG blending on PLCL degradation

The EGCG release profiles were examined to determine whether EGCG could be released from E-PLCL in amounts necessary to generate effective concentrations that inhibit the behaviors of VSMCs. As shown in Fig. 2A, EGCG was released in a logarithmic manner, in which the release rate decreased with time. A minor burst effect of less than 6% was observed during the first day of release. E-PLCL sustainedly released approximately 30% of blended EGCG during the first 30 days. This release profile is characteristic of diffusion controlled systems. From the release profile, it was found that about 110 μM EGCG was cumulatively released from E-PLCL for 3 days.

In vitro PLCL degradation was investigated by measuring MW change and mass loss. The MW of PLCL could be determined by GPC, however the MW of E-PLCL could not be measured due to adsorption of EGCG to the GPC columns. As shown in Fig. 2B, the MW was 10% of initial value after 1week and approximately 60% of the initial value after 8 weeks. However, the mass loss of PLCL was insignificant, during test periods (Fig. 2C). The MWs decreased to a larger extent than the change of mass loss, which is typical for such aliphatic polyesters. Aliphatic polyesters such as PGA, PLA and PCL are degraded by non-enzymatic random hydrolytic scission of esters linkage. The mass of E-PLCL gradually decreased until 6 weeks, but its mass loss accelerated at 8 weeks to approximately 4% loss of the initial weight (Fig. 2C). These results indicate that the mass loss of E-PLCL during incubation might be due to the release of EGCG from PLCL matrices. The EGCG release profile closely matches that of E-PLCL mass loss, suggesting that the main release mechanism during the test period might be diffusion, rather than polymer degradation.

3.3. Migration and invasion of VSMCs onto E-PLCL

The *in vitro* wound healing migration assay, created from a scrape wound in a confluent cell monolayer, was used to assess the effect of EGCG released from E-PLCL on VSMC migration. After scrape wounding, the behaviors of VSMC in the conditioned media obtained from either PLCL or E-PLCL were monitored. The initial denuded area onto PLCL was 1.43 ± 0.21 mm^2. With conditioned media from PLCL, the first evidence of cell ingrowth did not appear until around 24 h. Some parts of a scrape started to recover by 48 h after denuding (data not shown). After 72 h the denuded space was well filled in with cells indicating that scrape recovery was nearly complete (Fig. 3A). Since the doubling time for VSMCs with FBS stimulation is about 44 h, the commencement of the recovery with conditioned media from PLCL at 48 h implies that the cells had extensively migrated from the edge of the scrape into the denuded space immediately after the onset of cell proliferation. On the contrary, the denuded area closure in FBS-induced VSMCs with conditioned media from E-PLCL was completely suppressed after 72 h (Fig. 3A). The denuded area remained unpopulated until 48 h, even though a few cells at the edge of the scrape showed some forward movement (data not shown). VSMCs with conditioned media from E-PLCL showed neither migration nor ingrowth even after the onset of cell proliferation. The unrecovered area of scrape in VSMCs with conditioned media from PLCL and that from E-PLCL after 72h were 0.2±0.2 mm^2 and 1.32±0.2 mm^2, respectively. While about 14% of the initially denuded area remained uncovered after 72 h in VSMCs with conditioned media from PLCL, the cells with conditioned media from E-PLCL covered only 8% of the initial area. There was significant ($p < 0.05$) difference in the uncovered area between the cells with conditioned media from PLCL and E-PLCL after 72 h.

To determine whether EGCG released from E-PLCL affects VSMC invasion through extracellular matrices or not, a modified Boyden chamber assay was performed. Conditioned

media from E-PLCL completely suppressed the invasion of VSMCs after 72 h despite FBS stimulation, whereas most of the cells with conditioned media from PLCL invaded through extracellular matrices in response to FBS (Fig. 3B). The number of cells that had invaded across the reconstituted basement membrane was 121.4 ±8.6 and 116.8±9.0 for conditioned media from PLCL and fresh media, respectively. However when conditioned media from E-PLCL was used only 21.2 ±2.8 cells had invaded across the membrane. These results indicate that EGCG released from E-PLCL significantly ($p < 0.05$) inhibits VSMC invasion for at least 72 h. These results suggest that EGCG released from E-PLCL may be effective in inhibiting the migration of VSMCs across a thin layer as well as their invasion through a thick layer.

3.4. Adhesion and activation of platelets onto E-PLCL

The anti-thrombotic effects of E-PLCL were examined by assaying platelet adhesion and activation. Fig. 4A showed the morphologies of platelets adhered onto the surfaces of PLCL and E-PLCL films. The platelets adhered onto PLCL film were spread and had developed characteristic pseudopodia, which were typical morphologies of the activated states. Onto E-PLCL, however, platelet adhesion and aggregation were remarkably reduced with neither extension of pseudopodia nor deformation. The platelets adhered onto E-PLCL film were generally singular with a rounded shape. This morphology is typical of inactivated states. Moreover, the average number of platelets adhered on the different films was counted from SEM images (×1000). The number of platelets adhered onto PLCL films was 49.1±10.98 and that onto E-PLCL films was 11.1±2.91. After EGCG was incorporated into PLCL films, the number of adherent platelets significantly ($p < 0.05$) decreased. The activation of platelets leads to a rapid change of platelet morphology with formation of pseudopodia, spreading and

the onset of release reaction, followed by platelet aggregation [22]. P-selectin is present on the surface of activated platelets or released into plasma, and thus may be used as a marker of platelet activation onto biomaterials [22,23]. The amount of P-selectin released by platelets activated by E-PLCL was 84.7 % of the amount released by platelets adherent to PLCL ($p < 0.05$), suggesting that platelet activation was suppressed by EGCG when incubated in human plasma (Fig 4B). These results suggest that EGCG might improve the blood compatibility of PLCL via reducing platelet adhesion and activation.

3.5. Surface morphology and structural integrity of EGCG-eluting stents

Apart from pharmacokinetic requirements, polymer coatings containing a drug on metallic stents have to remain adherent and undamaged during stent implantation and expansion. For DES, surface topography is considered an important determinant of the bare stent performance. If the stent has webbings and bridges between the struts, the coating may break off from the stent when the stent is dilated by a balloon catheter. Thrombus and VSMC proliferation can occur at the site where the coating breaks off [22,24]. E-PLCL layers were able to mask impurities of bare stents and to smooth the surface, with uniform distribution over both exterior and interior surfaces (Fig. 5A). There were no cracks or webbings between struts after balloon-expansion. A smooth surface coating can significantly decrease injury to blood vessels. Furthermore, a smooth stent surface is believed to reduce platelet activation and aggregation, consequently leading to less thrombus formation and neointimal proliferation [22]. It was also found that the structural integrity of the stent coatings was maintained without delamination or destruction after 90% dilatation by an angioplasty balloon (Fig. 5B). This indicates that the stent coating has rubber-like elasticity and is sufficiently flexible to allow balloon expansion of the stent without cracking or peeling from

the struts. A close fit of the polymer layer around the stent strut is essential for maintaining structural integrity of the coated stents during crimping and dilatation. Thus, it seemed that E-PLCL coatings enable EGCG-eluting stents to withstand compressive and tensile strains without cracking in the stent expansion process.

4. Discussion

It is likely that local delivery of anti-proliferative, anti-migratory anti-thrombotic and anti-inflammatory drugs can prevent stent restenosis [25,26]. The principle hereby investigated was the application of a polymer coating as a vehicle for drug delivery, rather than to study a specific stent. In the present study, E-PLCL copolymers were prepared with uniformly dispersed EGCG as shown in FT-IR spectrum (Fig. 1C). Moreover, E-PLCL has been shown to have good physicochemical properties such as stable Tm, improved hydrophilicity and sustained release of EGCG (Figs. 1B and 2A). The degradation of PLCL implicated that a reduction of the polymer chain length by random cleavage of ester bonds, without the formation of soluble components, occurred during the experimental time period (Figs. 2B and 2C). After the drug elutes from the polymer coating, the residual synthetic polymer coating may lead to complications such as an exaggerated inflammatory response and neointimal hyperplasia at the implant site. The initial rationale of applying biodegradable polymeric coatings to intravascular stents has been to provide a biologically inert carrier and to have proper degradation rate. After a stent coating has released the drug it should degrade promptly. According to the EGCG release test and the polymer degradation test, PLCL degrades minimally during the initial 8 week controlled release phase but might degrade gradually after it has finished releasing EGCG. Additionally, these physicochemical characteristics and the degradation rate of PLCL can be easily controlled by adjusting the

ratio of lactide and caprolactone. Compared to other anti-proliferative and/or immune-suppressive agents utilized in DES, such as paclitaxel, sirolimus and curcumin [27–29], EGCG has several advantages. First of all, EGCG is biologically safe. It has been shown to have no dermal, acute, reproductive or short-term toxicity, teratogenicity or genotoxicity at physiological concentrations [30–32]. The biological safety of other drugs has not been fully elucidated yet. Second, it exerts differential dose-dependent migration-inhibitory activity in VSMCs vs. vascular endothelial cells. EGCG-mediated inhibition of proliferation and migration was found to occur at much higher dose of EGCG in endothelial cells as compared to VSMCs [33]. Third, it is effective enough to function at relatively low concentrations. EGCG was initially loaded into PLCL at a concentration of 5 wt% (approx. 1100 μmol/film), but by 3 days only 110 μM of EGCG had been released (Fig. 2C). The amount is sufficient to completely inhibit VSMC migration and invasion. Moreover, our previous report demonstrated that EGCG inhibited the proliferation and migration of serum-stimulated VSMCs and induced cell cycle arrest by down-modulating nuclear factor-κB [17].

The abnormal growth of VSMCs and their excess migration from the tunica media to the subendothelial region plays an important role in vascular diseases, including atherosclerosis and restenosis after angioplasty or stenting [34]. A number of studies have demonstrated that EGCG inhibits the behaviors of VSMCs induced by serum or growth factors [35,36]. In this study, it has been demonstrated that EGCG, released from E-PLCL, inhibits the migration and invasion of VSMCs (Fig. 3). It has been also shown that the inhibitory effects of EGCG are due to its structure with the galloyl group in the 3-position and abundant hydroxyl groups [36–38]. There is evidence that this EGCG-mediated inhibition might be ascribed to the adsorption of EGCG at specific sites on the cellular membrane or DNA that affects the cell proliferation and DNA replication [39,40]. Moreover, a recent study has demonstrated that expression of the metastasis-associated 67 kDa laminin receptor (67 LR) might confer EGCG

responsiveness to cancer cells at physiologically relevant concentrations. This suggests that the gallate moiety of EGCG may be critical for 67 LR binding and subsequent activity [41]. The observation that nucleic acids extracted from catechin-treated cells were colored, implies that both galloyl and catechol groups of EGCG are essential for DNA binding, and both groups seemed to hold strands of DNA via their branching structure [42]. These results suggest that EGCG may bind to specific receptors onto membranes, be internalized into the cytosol and further be translocated into the nucleus. This leads to the interruption of the exogenous signals directed to genes responsible for cellular responses including proliferation, migration and invasion of VSMCs.

Biocompatibility of cardiovascular grafts is often evaluated by the deposition of platelets and their activation. Platelet adhesion and activation occur during cardiopulmory bypass, hemodialysis and implantation of vascular grafts or stents. This may induce early thrombosis and late intimal hyperplasia [43]. In this study, incubating PLCL films with PRP from fresh whole human blood, resulted in platelet adhesion and activation, as measured by morphology change, adhered number and released CD62. Platelet adhesion mainly depends on the types and conformation of adsorbed plasma proteins. However, EGCG blending resulted in a significant decrease in platelet adhesion and activation onto PLCL as shown by reduced number and decreased P-selectin release (Fig. 4). Plasma protein adsorption onto polymers strongly depends on their surface characteristics such as hydrophobicity or charge. Hydrophobic surfaces have been shown to be more suitable to protein adsorption than hydrophilic surfaces [44]. Therefore, enhanced hydrophilicity of PLCL by EGCG addition could inhibit the protein adsorption by reducing the interfacial free energy. Proteins attached onto E-PLCL might be difficult to undergo conformation change, and thus fewer integrated locations of platelet would be exposed and few platelets would be activated [43]. It has been reported that EGCG could inhibit platelet aggregation induced by thrombin, collagen, and

thrombospondin-1. Moreover, EGCG shows an antithrombotic activity that inhibit cytoplasmic Ca^{2+} increase and thromboxane A_2 (TXA_2) formation through the inhibition of arachidonic acid liberation and TXA_2 synthase [45–47]. This inhibitory activity seems to be attributed to the structure with the galloyl group in the 3-position of EGCG as well as its antioxidant activity.

5. Conclusion

These findings provide support to a scenario in which EGCG released from biodegradable copolymers plays a key role in the inhibition of VSMC migration and invasion as well as the suppression of platelet adhesion and activation. Therefore, it is suggested that EGCG-releasing polymers can be potentially applied for fabricating an EGCG-eluting vascular stent, in order to prevent in-stent restenosis and thrombosis.

Figure captions

Figure 1. Physicochemical properties of EGCG-releasing PLCL (E-PLCL) copolymers. A) SEM micrographs (× 200) of PLCL and E-PLCL films, B) DSC profiles of PLCL and E-PLCL (the insert for EGCG) and C) FT-IR spectrum of PLCL and E-PLCL.

Figure 2. EGCG release from E-PLCL and effects of EGCG blending on PLCL degradation. A) *In vitro* release profile of EGCG from E-PLCL film, B) Molecular weight change (*in vitro* degradation) of PLCL and C) Cumulative weight loss of PLCL and E-PLCL films.

Figure 3. Effect of EGCG released from E-PLCL on serum-stimulated VSMC migration and invasion. A) Microscopic photographs (× 25) of cells migrated into denuded areas. A small scrape was made across a confluent monolayer, and then the process of denuded area closure was monitored for up to 72 h in the presence of conditioned media from PLCL or E-PLCL. B) Microscopic photographs (× 100) of cells invaded through matrigel and stained with toluidene blue. A modified Boyden chamber assay was used with matrigel-coated transwell inserts. Cells were incubated in the inner chamber of transwell with conditioned media from PLCL or E-PLCL for 72 h. The photographs shown in these figures are representative of 6 independent experiments, showing similar results.

Figure 4. Effect of EGCG released from E-PLCL on platelet adhesion and activation. A) SEM micrographs (× 300 and × 1,000) of adhered platelets. PRP isolated from human whole blood was incubated with PLCL and E-PLCL films for 2 h and then observed by SEM. The micrographs shown in this figure are representative of 6 independent experiments, showing similar results. B) Platelet activation was determined by detecting P-selectin (CD62), as

described in Materials and Methods. The results are reported as a mean ± SD (n = 6) and analyzed by the Bonferroni test. There is significant difference ($p < 0.05$) between CD62 activation by incubation with PLCL and E-PLCL.

Figure 5. Surface morphology and structural integrity of EGCG-eluting stents. A) Optical microscopic photos (× 75 and × 200) of an EGCG-eluting stent before and after balloon-expansion. B) SEM micrographs (× 50 and × 500) of an EGCG-eluting stent after balloon-expansion (An arrow indicates the struts of the stent).

References

[1] Lau KW, Mak KH, Hung JS, Sigwart U. Clinical impact of stent construction and design in percutaneous coronary intervention. Am Heart J 2004;147(5):764–73.

[2] Toutouzas K, Colombo A, Stefanadis C. Inflammation and restenosis after percutaneous coronary interventions. Eur Heart J 2004;25(19):1679–87.

[3] Finkelstein A, McClean D, Kar S, Takizawa K, Varghese K, Baek N, et al. Local drug delivery via a coronary stent with programmable release pharmacokinetics. Circulation 2003;107(5): 777–84.

[4] Babapulle MN, Joseph L, Belisle P, Brophy JM, Eisenberg MJ. A hierarchical Bayesian meta-analysis of randomised clinical trials of drug-eluting stents. Lancet 2004;364(9434):583–91.

[5] van der Hoeven BL, Pires NM, Warda HM, Oemrawsingh PV, van Vlijmen BJ, Quax PH, et al. Drug-eluting stents: results, promises and problems. Int J Cardiol 2005;99(1): 9–17.

[6] Acharya G, Park K. Mechanisms of controlled drug release from drug-eluting stents. Adv Drug Deliv Rev 2006;58(3):387–401.

[7] De Scheerder IK, Wilczek KL, Verbeken EV, Vandorpe J, Lan PN, Schacht E, et al. Biocompatibility of polymer-coated oversized metallic stents implanted in normal porcine coronary arteries. Atherosclerosis 1995;114(1):105–14.

[8] Rechavia E, Litvack F, Fishbien MC, Nakamura M, Eigler N. Biocompatibility of polyurethane-coated stents: tissue and vascular aspects. Cathet Cardiovasc Diagn 1998;45(2): 202–7.

[9] Costa MA, Simon DI. Molecular basis of restenosis and drug-eluting stents. Circulation 2005;111(17) 2257–73.

[10] Jaffe R, Strauss BH. Late and very late thrombosis of drug-eluting stents: evolving concepts and perspectives. J Am Coll Cardiol 2007;50(2)119–27.

[11] Tipoe GL, Leung TM, Hung MW, Fung ML. Green tea polyphenols as an anti-oxidant and anti-inflammatory agent for cardiovascular protection. Cardiovasc Hematol Disord Drug Targets 2007;7(2):135–44.

[12] Hofmann CS, Sonenshein GE. Green tea polyphenol epigallocatechin-3 gallate induces apoptosis of proliferating vascular smooth muscle cells via activation of p53. FASEB J 2003;17(6):702–4.

[13] Ivanov V, Roomi MW, Kalinovsky T, Niedzwiecki A, Rath M. Anti-atherogenic effects of a mixture of ascorbic acid, lysine, proline, arginine, cysteine, and green tea phenolics in human aortic smooth muscle cells. J Cardiovasc Pharmacol. 2007;49(3):140–5.

[14] Neuhaus T, Voit S, Lill G, Vetter H, Schrör K, Weber AA. Platelet aggregation induced by the C-terminal peptide of thrombospondin-1 (4N1-1) is inhibited by epigallocatechin gallate but not by prostaglandin E1. Platelets 2004;15(7):455–7.

[15] Jeong SI, Kim BS, Kang SW, Kwon JH, Lee YM, Kim SH, et al. In vivo biocompatibilty and degradation behavior of elastic poly(L-lactide-*co*-ε-caprolactone) scaffolds. Biomaterials 2004;25(28):5939–46.

[16] Piao H, Kwon JS, Piao S, Sohn JH, Lee YS, Bae JW, et al. Effects of cardiac patches engineered with bone marrow-derived mononuclear cells and PGCL scaffolds in a rat myocardial infarction model. Biomaterials 2007;28(4):641–9.

[17] Han D-W, Lim HR, Baek HS, Lee MH, Lee SJ, Hyon S-H, et al. Inhibitory effects of epigallocatechin-3-*O*-gallate on serum-stimulated rat aortic smooth muscle cells via NF-κB down-modulation. Biochem Biophys Res Commun 2006;345(1):148–55.

[18] Orlandi A, Ferlosio A, Gabbiani G, Spagnoli LG, Ehrlich PH. Phenotypic heterogeneity influences the behavior of rat aortic smooth muscle cells in collagen lattice. Exp Cell Res 2005;311(2):317–27.

[19] Galis ZS, Johnson C, Godin D, Magid R, Shipley JM, Senior RM, et al. Targeted disruption of the matrix metalloproteinase-9 gene impairs smooth muscle cell migration and geometrical arterial remodeling. Circ Res 2002;91(9):852–9.

[20] Basu A, Kligman LH, Samulewicz SJ, Howe CC. Impaired wound healing in mice deficient in a matricellular protein SPARC (osteonectin, BM-40), BMC Cell Biol. 2001;2:15.

[21] Cheng XW, Kuzuya M, Nakamura K, Liu Z, Di Q, Hasegawa J, et al. Mechanisms of the inhibitory effect of epigallocatechin-3-gallate on cultured human vascular smooth muscle cell invasion. Arterioscler Thromb Vasc Biol 2005;25(9):1864–70.

[22] Pan ChJ, Tang JJ, Weng YJ, Wang J, Huang N. Preparation, characterization and anticoagulation of curcumin-eluting controlled biodegradable coating stents. J Control Release 2006;116(1):42–9.

[23] Su SH, Nguyen KT, Satasiya P, Greilich PE, Tang L, Eberhart RC. Curcumin impregnation improves the mechanical properties and reduces the inflammatory response associated with poly(L-lactic acid) fiber. J Biomater Sci Polym Ed 2005;16(3):353–70.

[24] Dibra A, Kastrati A, Mehilli J, Pache J, von Oepen R, Dirschinger J, et al. Influence of stent surface topography on the outcomes of patients undergoing coronary stenting: a randomized double-blind controlled trial. Catheter Cardiovasc Interv 2005;65(3):374–80.

[25] Htay T, Liu MW. Drug-eluting stent: a review and update. Vasc Health Risk Manag 2005;1(4):263–76.

[26] Stone GW, Moses JW, Ellis SG, Schofer J, Dawkins KD, Morice MC, et al. Safety and efficacy of sirolimus- and paclitaxel-eluting coronary stents. N Engl J Med 2007;356(10):998–1008.

[27] de Lezo JS, Medina A, Pan M, Delgado A, Segura J, Pavlovic D, et al. Rapamycin-eluting stents for the treatment of unprotected left main coronary disease. Am Heart J 2004;148(3):481–5.

[28] Kastrati A, Dibra A, Eberle S, Mehilli J, Suarez de Lezo J, Goy JJ, et al. Sirolimus-eluting stents vs paclitaxel-eluting stents in patients with coronary artery disease: meta-analysis of randomized trials. JAMA 2005;294(7):819–25.

[29] Nguyen KT, Shaikh N, Shukla KP, Su SH, Eberhart RC, Tang L. Molecular responses of vascular smooth muscle cells and phagocytes to curcumin-eluting bioresorbable stent materials. Biomaterials 2004;25(23):5333–46.

[30] Isbrucker RA, Bausch J, Edwards JA, Wolz E. Safety studies on epigallocatechin gallate (EGCG) preparations. Part 1: genotoxicity. Food Chem Toxicol 2006;44(5):626–35.

[31] Isbrucker RA, Edwards JA, Wolz E, Davidovich A, Bausch J. Safety studies on epigallocatechin gallate (EGCG) preparations. Part 2: dermal, acute and short-term toxicity studies. Food Chem Toxicol. 2006;44(5):636–50.

[32] Isbrucker RA, Edwards JA, Wolz E, Davidovich A, Bausch J. Safety studies on epigallocatechin gallate (EGCG) preparations. Part 3: teratogenicity and reproductive toxicity studies in rats. Food Chem Toxicol 2006;44(5):651–61.

[33] Chung JH, Lim HR, Lee TH, Lee MH, Baek HS, Woo YI, et al. Growth of smooth muscle cell and endothelial cell on PLGA film containing EGCG. Key Eng. Mater. 2007;342-3:93–6.

[34] Linde J, Strauss BH. Pharmacological treatment for prevention of restenosis. Expert Opin Emerg Drugs 2001;6(2):281–302.

[35] Hofmann CS, Sonenshein GE. Green tea polyphenol epigallocatechin-3 gallate induces apoptosis of proliferating vascular smooth muscle cells via activation of p53. FASEB J 2003;17(6)702–4.

[36] Cheng XW, Kuzuya M, Nakamura K, Liu Z, Di Q, Hasegawa J, et al. Mechanisms of the inhibitory effect of epigallocatechin-3-gallate on cultured human vascular smooth muscle cell invasion. Arterioscler Thromb Vasc Biol 2005;25(9):1864–70.

[37] Isemura M, Saeki K, Kimura T, Hayakawa S, Minami T, Sazuka M. Tea catechins and related polyphenols as anti-cancer agents. Biofactors 2000;13(1-4):81–5.

[38] Sachinidis A, Skach RA, Seul C, Ko Y, Hescheler J, Ahn H-Y, et al. Inhibition of the PDGF β-receptor tyrosine phosphorylation and its downstream intracellular signal transduction pathway in rat and human vascular smooth muscle cells by different catechins. FASEB J 2002;16(8):893–5.

[39] Rodriguez SK, Guo W, Liu L, Band MA, Paulson EK, Meydani M. Green tea catechin, epigallocatechin-3-gallate, inhibits vascular endothelial growth factor angiogenic signaling by disrupting the formation of a receptor complex. Int J Cancer 2006;118(7):1635–44.

[40] Stangl V, Dreger H, Stangl K, Lorenz M. Molecular targets of tea polyphenols in the cardiovascular system. Cardiovasc Res 2007;73(2)348–58.

[41] Tachibana H, Koga K, Fujimura Y, Yamada K. A receptor for green tea polyphenol EGCG. Nat Struct Mol Biol 2004;11(4):380–1.

[42] Kuzuhara T, Sei Y, Yamaguchi K, Suganuma M, Fujiki H. DNA and RNA as new binding targets of green tea catechins. J Biol Chem 2006;281(25):17446–56.

[43] Zhou J, Yuan J, Zang X, Shen J, Lin S. Platelet adhesion and protein adsorption on silicone rubber surface by ozone-induced grafted polymerization with carboxybetaine monomer. Colloids Surf B Biointerfaces 2005;41(1):55–62.

[44] Tangpasuthadol V, Pongchaisirikul N, Hoven VP. Surface modification of chitosan films. Effects of hydrophobicity on protein adsorption. Carbohydr Res 2003;338(9):937–42.

[45] Deana R, Turetta L, Donella-Deana A, Donà M, Brunati AM, De Michiel L, et al. Green tea epigallocatechin-3-gallate inhibits platelet signalling pathways triggered by both proteolytic and non-proteolytic agonists. Thromb Haemost 2003;89(5):866–74.

[46] Son DJ, Cho MR, Jin YR, Kim SY, Park YH, Lee SH, et al. Antiplatelet effect of green tea catechins: a possible mechanism through arachidonic acid pathway. Prostaglandins Leukot Essent Fatty Acids 2004;71(1):25–31.

[47] Neuhaus T, Voit S, Lill G, Vetter H, Schrör K, Weber AA. Platelet aggregation induced by the C-terminal peptide of thrombospondin-1 (4N1-1) is inhibited by epigallocatechin gallate but not by prostaglandin E1. Platelets 2004;15(7):455–7.

Fig. 1

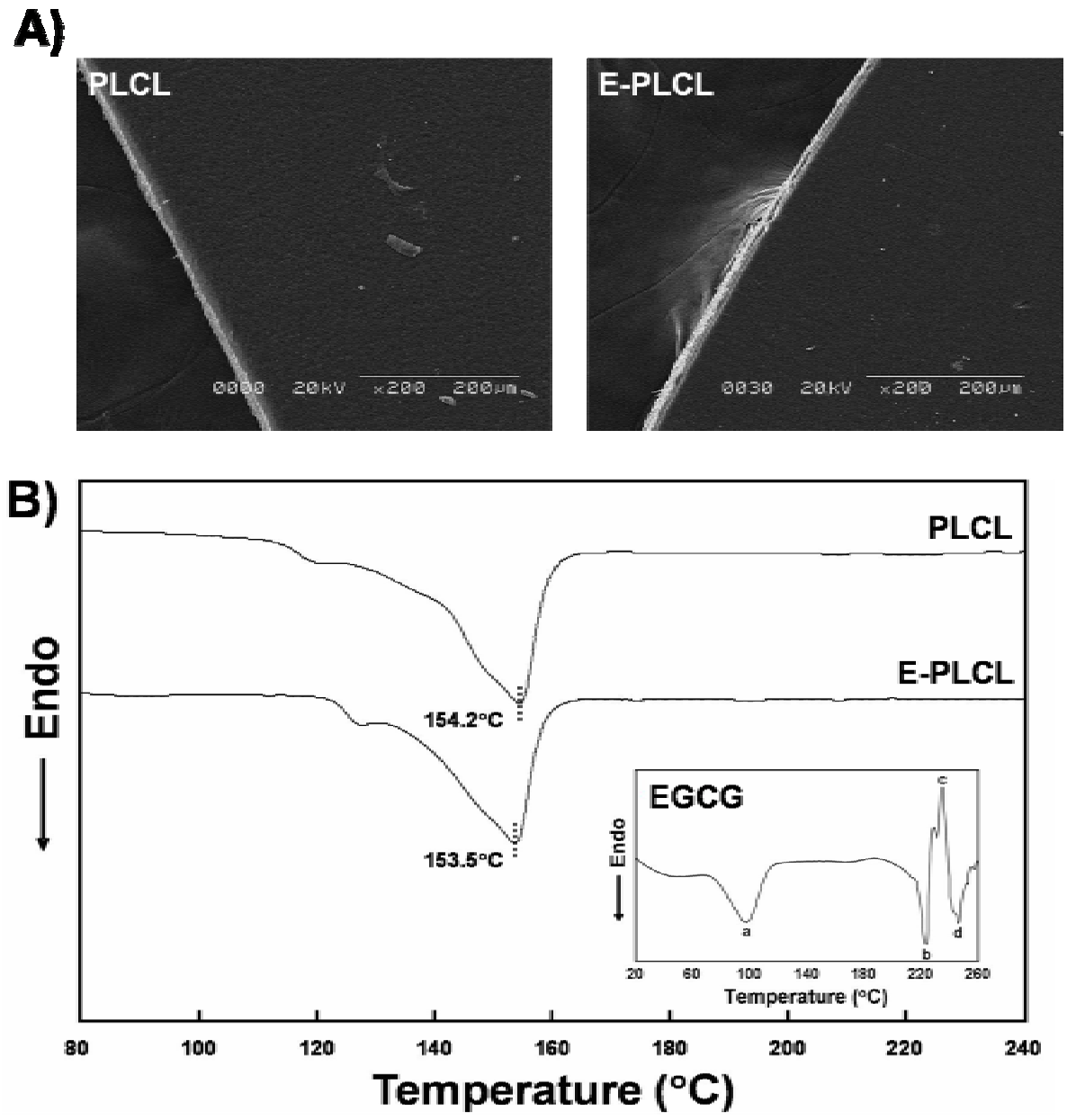
A)
PLCL
E-PLCL
0000 20kV ×200 200μm
0030 20kV ×200 200μm
B)
PLCL
E-PLCL
154.2°C
153.5°C
Endo
EGCG
Endo
a
b
c
d
20 60 100 140 180 220 260
Temperature (°C)
80 100 120 140 160 180 200 220 240
Temperature (°C)

C)

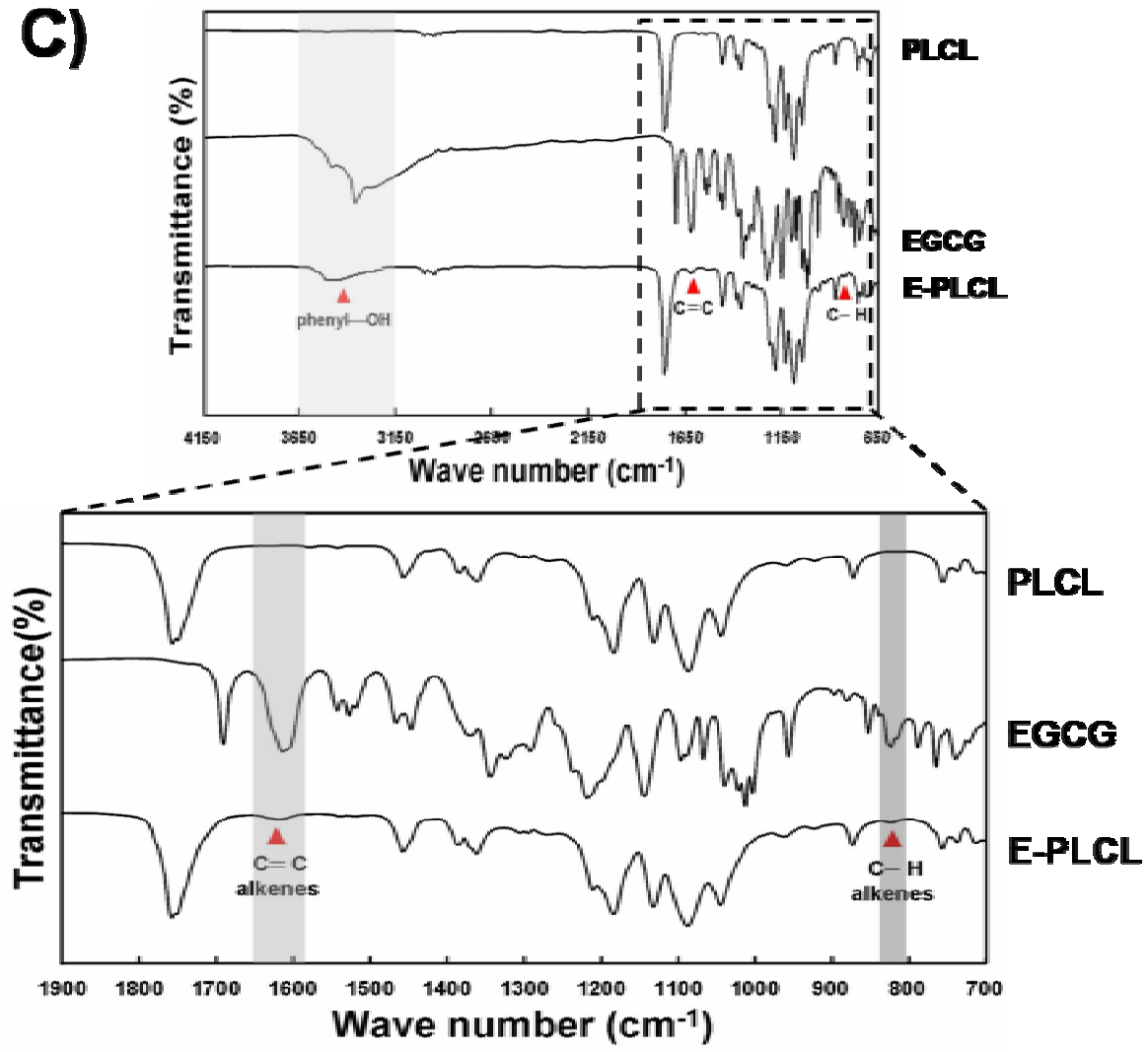
Transmittance (%)
PLCL
EGCG
E-PLCL
phenyl—OH
C=C
C— H
4150
3650
3150
2150
1650
1150
650
Wave number (cm-1)
Transmittance(%)
PLCL
EGCG
E-PLCL
C= C
alkenes
C— H
alkenes
1900
1800
1700
1600
1500
1400
1300
1200
1100
1000
900
800
700
Wave number (cm-1)

Fig. 2

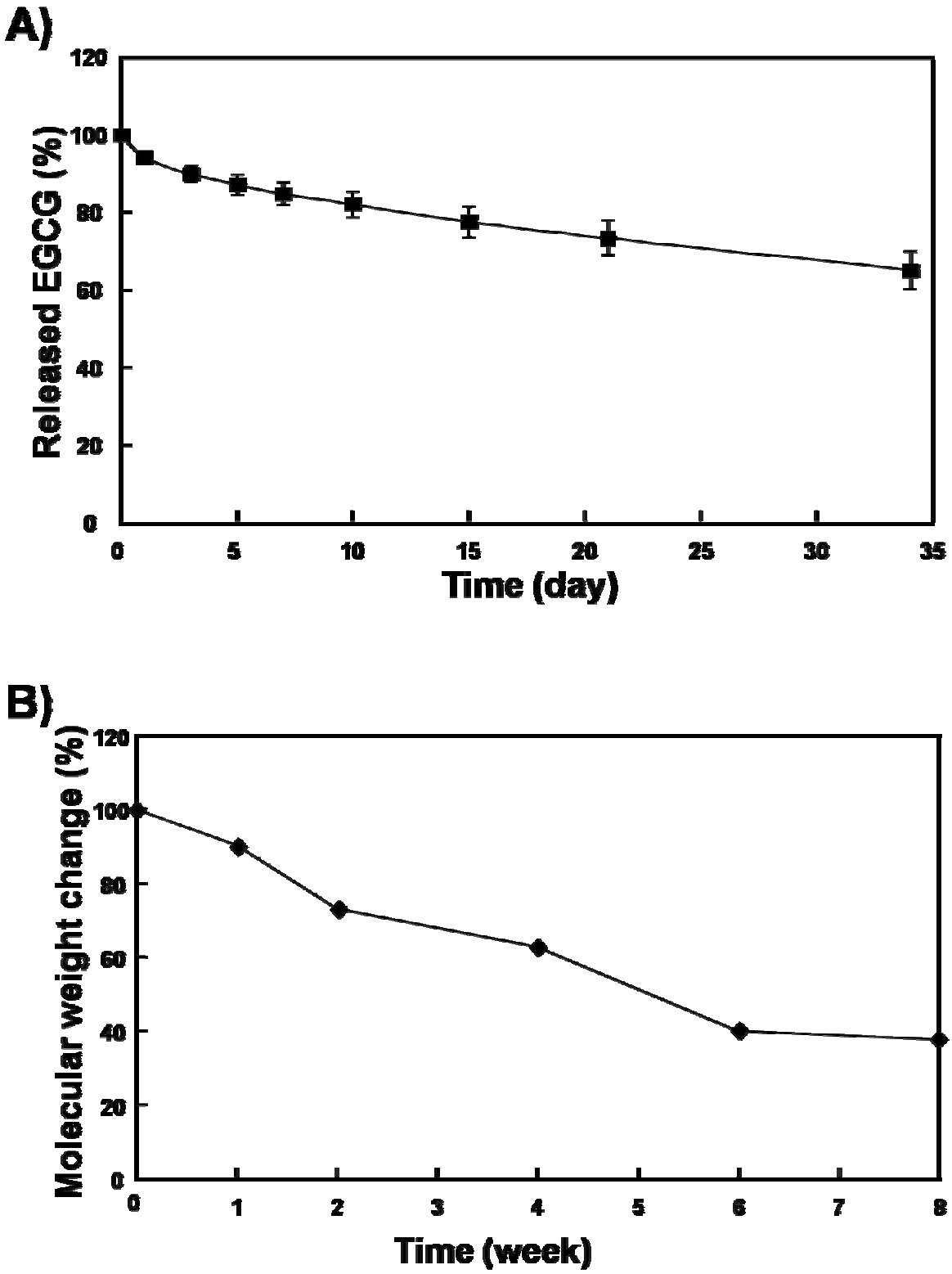
A)
Released EGCG (%)
120
100
80
60
40
20
0
0
5
10
15
20
25
30
35
Time (day)
B)
Molecular weight change (%)
120
100
80
60
40
20
0
0
1
2
3
4
5
6
7
8
Time (week)

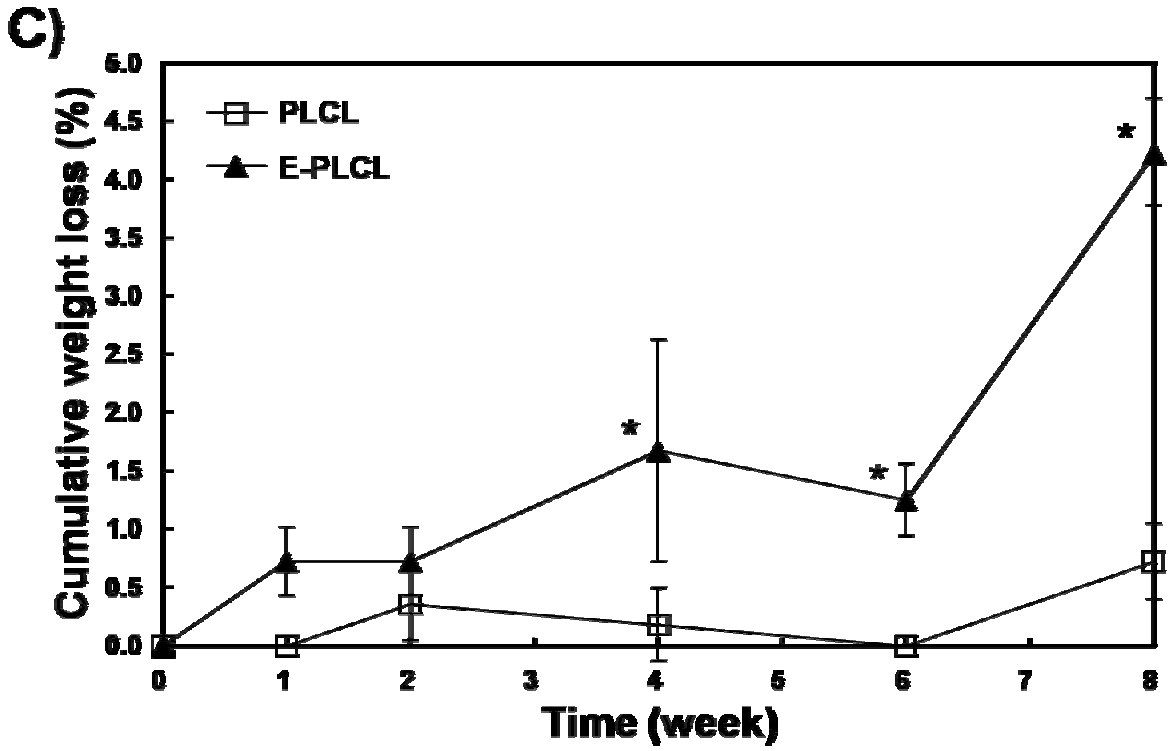
C)
Cumulative weight loss (%)
PLCL
E-PLCL
Time (week)
0.0
0.5
1.0
1.5
2.0
2.5
3.0
3.5
4.0
4.5
6.0
0
1
2
3
4
5
6
7
8
*
*
*

Fig. 3

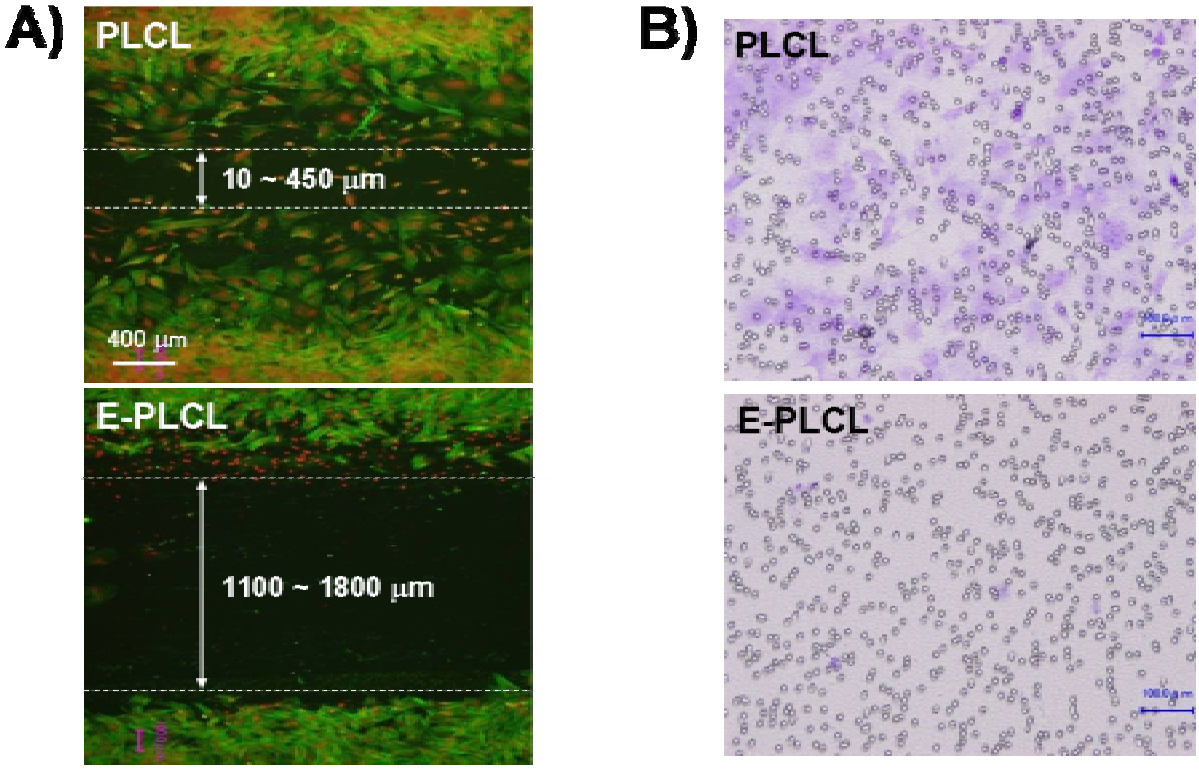
A)
PLCL
10 ~ 450 μm
400 μm
E-PLCL
1100 ~ 1800 μm
B)
PLCL
E-PLCL

Fig. 4

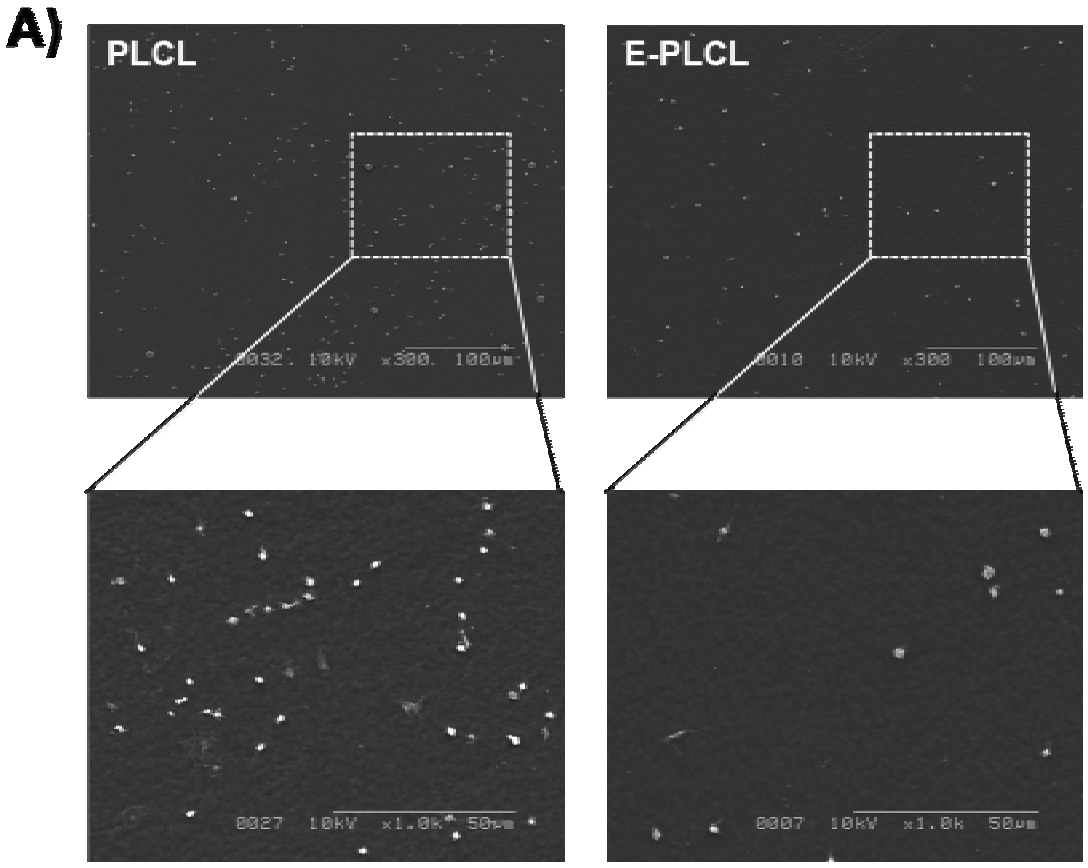
A)
PLCL
E-PLCL
0032 10kV x300 100μm
0010 10kV x300 100μm
0027 10kV x1.0k 50μm
0007 10kV x1.0k 50μm

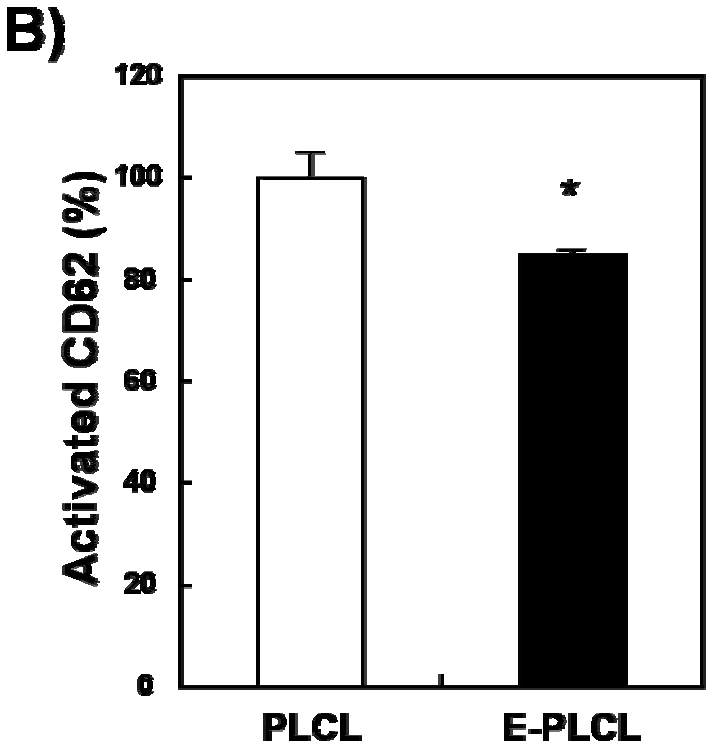
B)
Activated CD62 (%)
120
100
80
60
40
20
0
*
PLCL
E-PLCL

Fig. 5

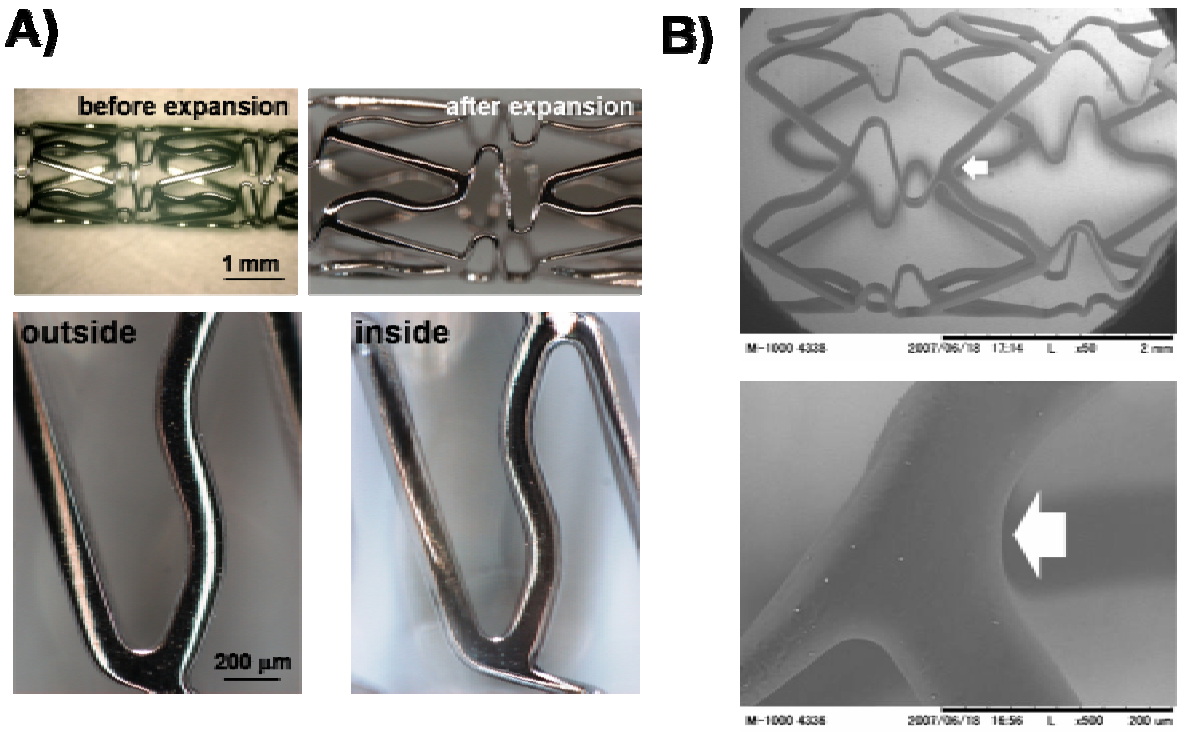
A)
before expansion
1 mm
after expansion
outside
200 µm
inside
B)